

# Provenance of loess from the Spanish central region: chemometric interpretation

R. GARCÍA\*†, M. D. PETIT-DOMÍNGUEZ‡, M. I. RUCANDIO§ & J. A. GONZÁLEZ¶

\*Departamento Geología y Geoquímica, Facultad de Ciencias, Universidad Autónoma, 28049 Madrid, Spain

‡Departamento Química Analítica, Facultad de Ciencias, Universidad Autónoma, 28049 Madrid, Spain

§Unidad de Espectroscopía, CIEMAT, 28040 Madrid, Spain

¶Departamento Geografía, Facultad de Filosofía y Letras, Universidad Autónoma, 28049 Madrid, Spain

(Received 2 April 2010; accepted 10 September 2010; first published online 2 December 2010)

**Abstract** – In this work our purposes are (1) geochemical characterization of loess ('primary loess' or 'true loess' and 'secondary loess' or 'loess-like deposits') located in the centre of the Iberian Peninsula, (2) systematic study of element behaviour during pedogenesis and (3) evaluation of the suitability of using the geochemistry of loess to establish the average composition of these discontinuous aeolian sedimentary covers in central Spain. Several analyses were carried out on the bulk sample and on the sandy and clay fractions (mineralogical composition by X-ray diffraction, mineralogical studies of heavy minerals by petrographical microscopy and chemical composition by flame atomic absorption spectrometry). Loess from the Spanish central region has a local origin. The presence of gypsum in the 'loess-like' deposits reaches values two times higher than in 'true loess', and 'true loess' has a higher concentration of quartz, calcite and kaolinite. Regarding chemical composition, similar concentrations of Ca, K, Mg and Na were found, although it is important to note the higher concentration of Na in some of the samples.

Keywords: loess, mineralogy, Tajo river valley, chemometric analysis, central Spain.

## 1. Introduction

Loessic accumulations are distributed in all continents around the world (Haase *et al.* 2007). Their geographical distribution, concentrated in two large latitudinal belts, confirms the local character of the morphogenetic processes that were able to mobilize fine materials: temperate regions, where 'cold loess' (Pecsi, 1990) or 'periglacial loess' (Frazee, Fehrenbacher & Krumbain, 1970) are the more abundant; and tropical flanks, on the edges of hyperarid regions, where 'desert loess' (Whalley, Marshall & Smith, 1982) is located. Outside of these zoned contexts, loess is located in the mountains ('mountain loess', Smalley, 1995 or 'perimontane loess', Pye, 1995) and in some fluvial basins of South American subtropical latitudes. They also appear in Mediterranean regions, where loess has a different texture, but they constitute a clear indicator of the presence of wind palaeoenvironments associated with a certain climatic Quaternary crisis, of a cold or dry type, that took place over their territories.

Dust records represent archives for palaeoclimatic change in terms of aridity in the source regions of the dust, palaeowind strengths, directions of palaeowind fields and precipitation frequency. However, there is no simple correlation between climate and dust transport (Grunert & Lehmkuhl, 2004). Silt-sized debris is the major particle fraction of loess. Mechanisms that produce silt particles include the direct release from parent rocks, glacial grinding,

fluvial and aeolian abrasion, crushing, and salt frost and chemical weathering (Pye, 1995). These mechanisms took place in habitual form in the past, and certain dust accumulation sites formed from varied source regions; even today the process continues. The particle flux from the Alpine mountain regions with high relief energy into dry lands is supposed to be the greatest primary supplier of clay and silt-sized debris for atmospheric transport.

In this sense, accumulations of loess were discovered in several places in Libya (Hey, 1972), the Atlas Mountain hillsides in Morocco (Coudé-Gaussen, 1991) and mainly in Tunisia, a few kilometres from the Mediterranean coast (Coudé-Gaussen, Hillaire-Marcel & Rognon, 1982). There, in the Matmata tablelands, are covers of loess 10–20 m thick (Coudé-Gaussen, Le Coustumer & Rognon, 1984; Coudé-Gaussen *et al.* 1987). This loess is composed of particles of silt 0.055–0.063 mm in diameter (thicker than periglacial loess) and it also contains a certain amount of clay (less than 25%). It is considered 'desert loess' or 'warm loess' (Pecsi, 1990) and originated in the past from the frequent sandstorms that took place in the Sahara. Even today sandstorms are able to sweep large amounts of powdered material away up to remote areas of northern and southern Europe, western areas of the Atlantic Ocean (Eberl & Smith, 2009) and even certain regions of South America (Goudie & Middleton, 2001).

In Tunisia, loess originated from silts swept away by western winds (Coudé-Gaussen, 1998). They are composed of allochthonous minerals like quartz

†Author for correspondence: rosario.garcia@uam.es

(30–65 %) and feldspars (5–25 %) and other minerals, with high fluctuations in concentrations of certain minerals such as calcite (5–55 %) (Coudé-Gaussen, Hillaire-Marcel & Rognon, 1982). But, in spite of their clear wind origin, a great controversy was created by some authors about their classification as ‘true loess’. This is due to the fact that they were accumulated under very different environmental conditions to the loess coming from cold regions. At the end of the 1960s, diverse lime silt accumulations were identified as ‘torrential loess’ in some regions of Mediterranean Spain such as Andalucía, Cataluña and País Valenciano (Brunnacker & Lözek, 1969; Brunnacker, 1969*a,b*). This loess type was located between 650 and 1000 metres above sea level going down to between 50 and 100 m in some places of Cataluña. It has been compared with Balkan loess, although analytical techniques were not used to confirm its textural and mineralogical characteristics. Its chronological age was determined by indirect procedures and correlation to the Würm glacial stage. Identical loess was later located on the Mediterranean coast of Spain (Alicante). It was not ‘typical loess’ from aeolian loess remobilized by stream waters and had a different grain size to the corresponding loess from the centre of Europe (Cuenca Payá & Walter, 1976). On the other hand, in the centre of Spain, a ‘loess-like’ type of deposit was located around the western foothills of the Toledo Mountains. Its origin was associated with ancient silts from the Würm stage that were mobilized by wind from the alluvial plains of the Záncara and Cigüela rivers and reworked later by water (A. Pérez González, unpub. Ph.D. thesis, Univ. Complutense, Madrid, 1982). In the same way, vast covers of wind-blown silts, associated with the Würm stage, were also located in the centre of Spain over different geomorphological units in bordering territories of Comunidad de Madrid and Castilla-La Mancha, and they were geomorphologically and sedimentologically analysed.

A couple of decades later, new deposits of loess were located in the north of the island of Mallorca (Spain). They were associated with very fine silt accumulations (with minimal amounts of sand and clay), constituted principally of silica and calcite and probably belonged to ancient materials accumulated during isotope stage 4 (67 000–45 000 BP) in very harsh environments with average annual temperatures of about 4.9 °C (Rose, Meng & Watson, 1999). Other deposits of loess (<10 m thick) were also located in the deep intermountain valleys of Granada, in the southwest of Spain, at 500–900 metres above sea level (Günster *et al.* 2001). This loess was remobilized by water and is composed of sand (2–22 %), silt (8–70 %) and clay (4–27 %). This loess is similar to those from the centre of Europe, though it has a higher affinity with Tunisian loess. Owing to it being fossilized in red soils dated as Eemian, it is related to recent Pleistocene steppes.

Recently, accumulations of ‘loess-like’ deposits have been located in some areas of the central Iberian

Peninsula, in the location of Mesa de Ocaña (Ruiz Zapata *et al.* 2000) and in a fluvial terrace of the Tajo River located in the surroundings of the city of Toledo (Pérez González *et al.* 2004).

According to the literature, the difference between ‘true loess’ and ‘loess-like’ deposits lies in their being considered to have either originated *in situ* or been remobilized, i.e. changed position, respectively. Small variations exist between the two. They differ scarcely in their physical properties and only geomorphology can make a difference; just a slightly larger particle size and a higher anisotropy resulting from the presence of certain fragments of detrital grains larger than sand. However, the geomorphological locations that are usually filled by both are different (R. García, unpub. Ph.D. thesis, Univ. Autónoma, Madrid, 2004).

The loess deposits that form the subject of this work have been studied before (García, Vigil, & González, 1998; García Giménez & González Martín, 2006; García *et al.* 2010; R. García, unpub. Ph.D. thesis, Univ. Autónoma, Madrid, 2004). These materials exhibit a remarkable originality in the European continent: accumulations and palaeoclimatic manifestations of a diverse nature (‘Grèzes litées’, ‘groizes’, loessic deposits, tuffaceous accumulations, crioturbations, etc.) are present in its territory and they were generated under an environment with temporal and spatial associations relatively rare in other domains.

Our purposes in this paper are the following: (1) A detailed geochemical characterization of loess. The variation among different loess strata should provide valuable information on the formation source and possible changes in main wind patterns. (2) Systematic study of element behaviour during pedogenesis. Abundances and ratios of oligoelements can be considered as primary features of the sediments, hence as tracers of their provenances (protolith indicator). By contrast, relative abundances of mobile elements may be related to the intensity of weathering/alteration processes, and thus they can be used as indicator of pedogenetic intensity (climatic proxy). (3) Evaluation of the suitability of using loess geochemistry to establish the average composition of the upper continental crust (Taylor, McLennan & McCulloch, 1983; Jin, You & Yu, 2009).

## 2. Morphostructural and bioclimatic context

The Madrid basin shows one of the most complex and interesting Quaternary sequences in all of Western Europe. Furthermore, among their different accumulations, numerous Pleistocene and Holocene silt materials and loess deposits have been found, especially located on the southern slope of the Tajo River (R. García, unpub. Ph.D. thesis, Univ. Autónoma, Madrid, 2004; García *et al.* 2010).

The study area is located in the middle Tajo River valley (central region of the Madrid basin) among the tablelands of Colmenar de Oreja, Chinchón to the north,

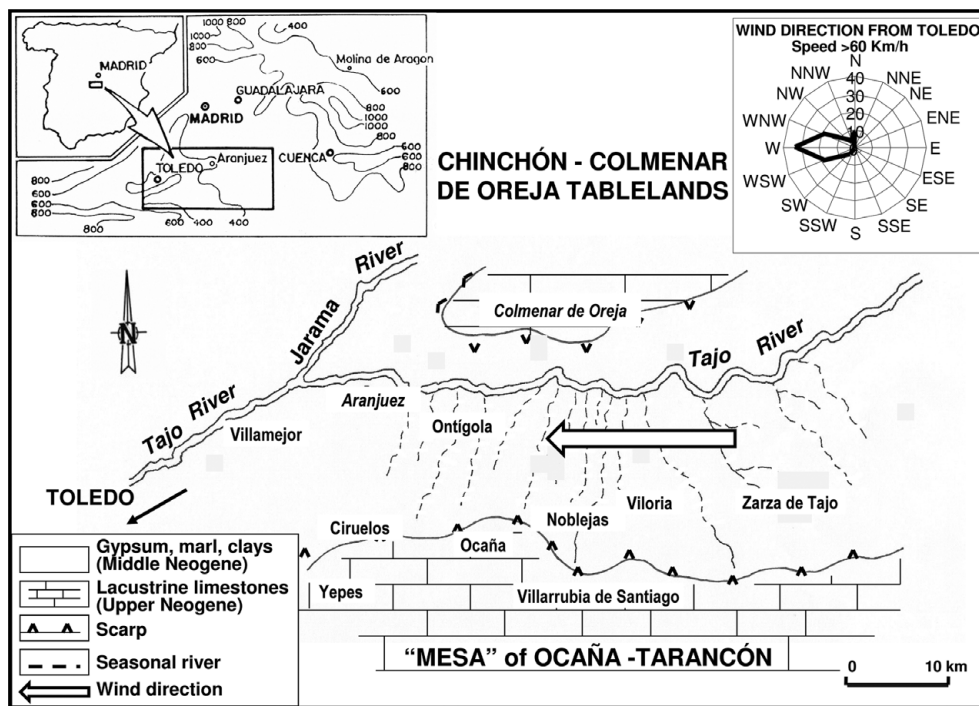


Figure 1. Location map showing geological units, wind directions and sampling zones.

and Mesa of Tarancón-Ocaña to the south, at a higher altitude of 500–1000 metres above sea level (Fig. 1). In this valley, sediments are composed of Neogene evaporites belonging to the ‘Miocene Lower Unit’ and the ‘Miocene Intermediate Unit’. At the top of the valley, these sediments transform into conglomerates and lacustrine limestones belonging to the ‘Miocene Upper Unit’ (Ordoñez, López-Aguayo & García del Cura, 1977). On this geological structure there are different geomorphological Pleistocene and Holocene units: terraces, alluvial fans, erosional and detrital glacia, colluviums, tuff deposits and silt accumulations that will be the subjects of this study.

This region has relatively cold and very dry winters as well as warm summers with moderate annual rainfalls. This region has a mild Mediterranean climate type ‘Csa’, with high evapotranspiration and droughts in summer.

The annual rainfalls are moderate (400–500 mm) and during the summer they are minimal and lead to the typical summer droughts of the Mediterranean climates: extremely harsh with a large and intense stress on vegetation. These peculiarities are controlled by a dynamic atmosphere, with presence of high pressures in summer and winter, which operate as a barrier against low pressures from the west. On the contrary, the highest rainfall values take place in the spring. With data from the Meteorological Observatory of Toledo (closest recording station to the area with complete data), a compass rose was constructed on which west-blowing winds are shown to be predominant in the region, which also follow the course of large rivers as indicated in Figure 1.

### 3. Materials and methods

#### 3.a. Materials

The analysed materials were collected from several profiles of the studied area and are composed of unstratified and massive clayey-silt, with varied amounts of calcium carbonate. Some of them are represented in Figure 2. Samples have been grouped according to their geographical locations (a – Viloría stream, b – Ciruelos, e – Villamejor, n – Noblejas, o – Mesa de Ocaña, t – Ontígola, x – Villarrubia de Santiago, y – Yepes, z – Zarza de Tajo). In addition, samples were also classified according to geomorphological criteria and their loessic characteristics as ‘true loess’, ‘loess-like’ or other unclassified samples (García Giménez & González Martín, 2006).

#### 3.b. Methods

Mineralogical analyses were carried out by x-ray diffraction (XRD) using the random powder method for the bulk sample and the oriented slides method for the < 2 µm fraction (Moore & Reynolds, 1997). A SIEMENS D-5000 x-ray diffractometer with a Cu anode was used, operating at 30 mA and 40 kV with divergence and reception slits of 2 and 0.6 mm, respectively. The procedure proposed by Schultz (1964) was used to quantify the components in the bulk sample. For the clay fraction (< 2 µm), oriented aggregates were air dried, glycolated with ethylene-glycol and heated at 550 °C for 2 hours. Semiquantitative mineralogical





Figure 2. (a) ‘True loess’ on the Miocene sediments. (b) ‘True loess’ preserving Miocene gypsums. (c) ‘True loess’ from the right side of the Tajo River. (d) Ancient cave dwelling (Troglodyte age) in the loess on the left side of the Tajo River. See <http://journals.cambridge.org/geo> for a colour version of this figure.

analysis was based on the diffraction peaks (Kisch, 1990).

Chemical analyses of major and minor elements were performed by flame absorption and emission spectrometry in a PERKIN ELMER 503 spectrometer. Previous dissolution of samples was carried out in the following way: a minimum amount of sample was treated with hydrofluoric acid in an open vessel and heated on a hot plate. It was followed by addition of aqua regia, heating again until dried. The residue was dissolved with 1 ml of concentrated hydrochloric acid and then diluted with water to the mark in Teflon volumetric flasks. Care was taken to keep the contamination to a minimum. Ultrapure water was used throughout and all reagents used were of analytical grade. In all flame absorption and emission spectroscopy determinations, blanks of reactive were analysed giving signals under the detection limits (García, Vigil & González, 1998). Element contents (Na, K, Ca, Mg, Al, Mn, Fe, Cu, Ti and Cr) were evaluated by means of the calibration curve for each element.

Light and heavy mineralogical fractions were separated by using bromoform (2.89 specific gravity). The lighter fraction remains floating on the surface while

the heavier one is deposited at bottom. Grains were identified through petrographical microscopy.

Finally a statistical processing of the data was carried out using the Statgraphics 5.0 program as will be explained in detail in the next Section.

#### 4. Results and discussion

From the point of view of grain size, a crucial factor in the classification of loess, the nine groups of studied materials are massive accumulations without internal structures, predominantly of silty clay loam texture (b, e, n, o, x, y & z groups), clay texture (a group) and fine silt (t group). It is notable that all deposits of the Mesa de Ocaña (o group) correspond to the ‘loess-like’ classification and that the samples collected in Ontígola (t) and Yepes (y) are all ‘true loess’ (García *et al.* 2010).

Mineralogical analyses were commonly used in sediment provenance studies (Biscaye *et al.* 1997). Our results indicate that quartz and gypsum are the most abundant minerals comprising about 50 % in the selected size fraction. Quartz, feldspars, gypsum, phyllosilicates, calcite and dolomite are the main minerals, representing more than 90 % of the total.

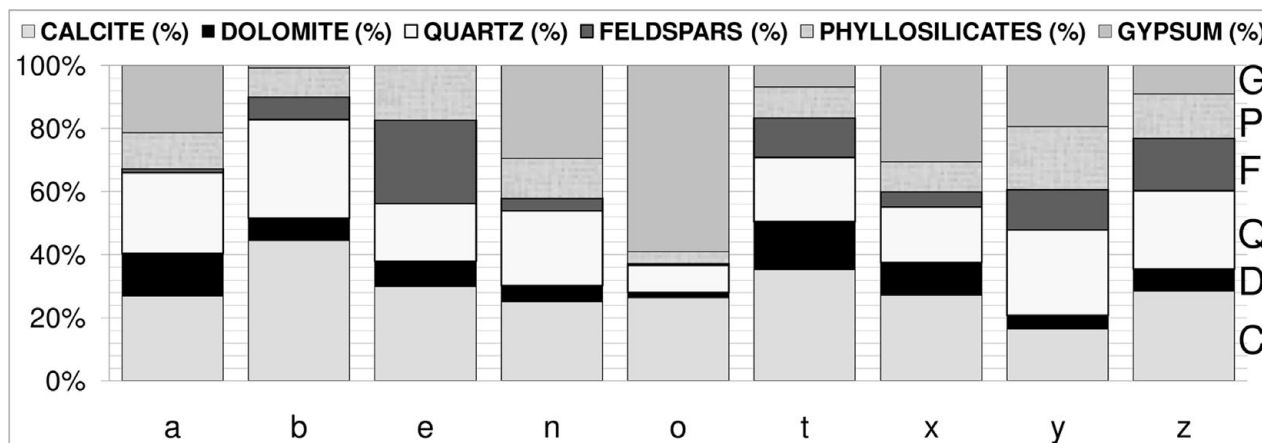


Figure 3. Mineralogical composition of the light minerals in each of the sample group locations (a – Vitoria stream; b – Ciruelos; e – Villamejor; n – Noblejas; o – Mesa de Ocaña; t – Ontígola; x – Villarrubia de Santiago; y – Yepes; z – Zarza de Tajo). See <http://journals.cambridge.org/geo> for a colour version of this figure.

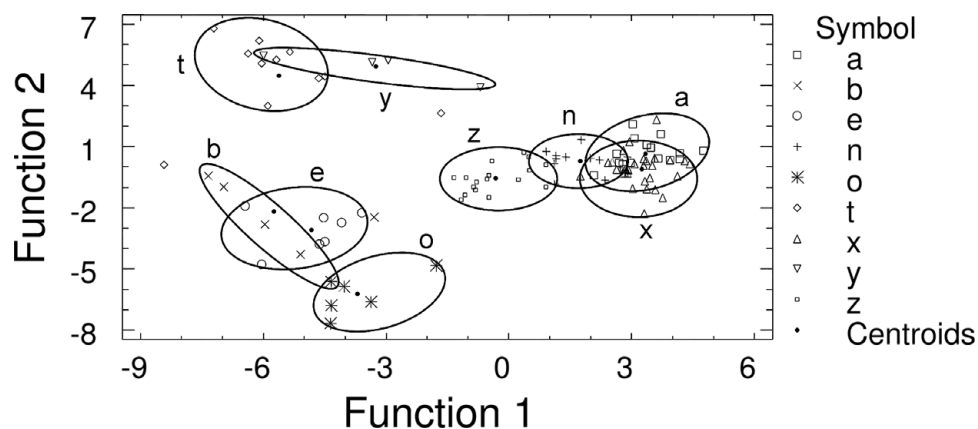


Figure 4. Mineralogical discriminant function of the nine sample groups analysed (a – Vitoria stream; b – Ciruelos; e – Villamejor; n – Noblejas; o – Mesa de Ocaña; t – Ontígola; x – Villarrubia de Santiago; y – Yepes; z – Zarza de Tajo). See <http://journals.cambridge.org/geo> for a colour version of this figure.

Figure 3 is a representation of the average content of the light minerals distributed in the nine sampling areas.

Considering the nine established groups, as a function of the geographical location, linear discriminant analysis was used for hard classification of mineral data, which provides a way to find possible connections among a high number of variables and classify samples into compositional groups sharing similar composition. For this study, 24 mineral variables (minerals of the bulk sample and clay and sandy fractions) were considered: calcite, dolomite, quartz, feldspars, phyllosilicates, gypsum, kaolinite, sepiolite, illite, smectite, tourmaline, zircon, garnet, apatite, brookite, rutile, fluorite, zoisite, anatase, staurolite, distene, sillimanite, opaque minerals and biotite. Figure 4 is a graphical representation of the samples as a function of the two canonical discriminant functions. F1 represents 45.91% of the variance and F2 22.89%. These functions with  $P$ -values less than 0.05 are statistically significant at the 95% confidence level. F1 and F2 have negative signs for calcite, dolomite, quartz, feldspars, phyllosilicates, garnet, staurolite and sillimanite; and

positive signs for sepiolite, tourmaline and biotite. The following variables have opposite signs: gypsum, kaolinite, illite, smectite, zircon, apatite, brookite, rutile, fluorite, zoisite, anatase, distene and opaque minerals.

Each category is well represented and it is characterized by a centroid (marked as  $\cdot$ ), which is the average for each group (unique value in the classification factor field). The samples belonging to each category (place) are grouped inside an enclosure. Figure 4 shows a clear difference among sample compositions from different locations. From a simple observation of the graphic, it can be observed that the nine groups of samples are in quite separate zones with few common zones among them. Samples from sites t and y are located in the positive axis of F2 and negative axis of F1. Groups b, e and o, are located in the negative axis of F1 and F2, group z is sited near the origin and groups n, a and x are located in the positive axis of F1 and near the zero value for F2. The groups a and x are rather mixed.

XRD analyses of the clay fraction showed tri-octahedral phyllosilicates with illite as the dominant clay mineral, originated from biotite alteration. It also

Table 1. Mineralogical composition of the heavy minerals in the sand fraction in each of the sample group locations (a – Viloría stream; b – Ciruelos; e – Villamejor; n – Noblejas; o – Mesa de Ocaña; t – Ontígola; x – Villarrubia de Santiago; y – Yepes; z – Zarza de Tajo)

	a	b	e	n	o	t	x	y	z
Tourmaline (%)	27.1	22.8	20.1	23.2	9.0	18.0	35.0	28.5	24.5
Zircon (%)	18.3	11.2	18.7	14.7	14.7	14.2	21.6	31.0	23.0
Garnet (%)	0.9	25.0	20.4	13.0	27.0	7.9	0.5	<0.1	16.6
Apatite (%)	<0.1	4.4	1.7	<0.1	<0.1	3.7	<0.1	<0.1	<0.1
Brookite (%)	<0.1	<0.1	<0.1	<0.1	3.5	<0.1	0.2	<0.1	<0.1
Rutile (%)	1.3	<0.1	<0.1	<0.1	0.5	<0.1	1.6	<0.1	<0.1
Fluorite (%)	<0.1	<0.1	<0.1	<0.1	<0.1	3.7	<0.1	6.0	<0.1
Zoisite (%)	8.3	<0.1	<0.1	4.3	0.0	4.0	2.8	3.0	0.6
Anatasa (%)	0.4	<0.1	<0.1	<0.0	6.7	6.1	2.5	3.0	2.6
Staurolite (%)	8.7	15.6	13.4	4.5	18.8	12.5	8.4	<0.1	8.1
Distene (%)	3.8	<0.1	<0.1	7.6	0.0	3.0	3.2	12.3	5.9
Sillimanite (%)	0.1	8.8	9.3	<0.1	5.5	4.2	<0.1	<0.1	<0.1
Opagues (%)	1.4	0.4	0.3	3.7	9.2	<0.1	1.4	<0.1	1.2
Biotite (%)	28.6	11.8	3.7	29.6	1.0	22.7	23.0	12.5	20.1

See <http://journals.cambridge.org/geo> for a graphical representation of this data.

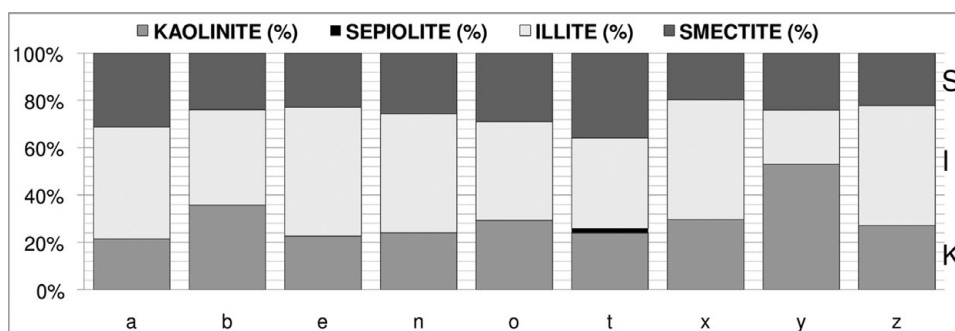


Figure 5. Mineralogical composition of the clay fraction in each of the sample group locations (a – Viloría stream; b – Ciruelos; e – Villamejor; n – Noblejas; o – Mesa de Ocaña; t – Ontígola; x – Villarrubia de Santiago; y – Yepes; z – Zarza de Tajo). See <http://journals.cambridge.org/geo> for a colour version of this figure.

identified smectite (in variable proportions) interstratified minerals at 10–14 Å and kaolinite (Fig. 5). The heavy minerals of the sand fraction are represented in the same way in Table 1, showing a wide variety of minerals with important contents of tourmaline, zircon, staurolite, garnet and biotite. Opaque minerals include magnetite, limonite and hematite. To obtain information about the environmental influences on the heavy minerals, the following ratios were calculated:  $K_1$  = chain silicates/epidotes,  $K_2$  = chain silicates/opaque minerals and  $K_3$  = epidotes/opaque minerals. Chain silicates, epidotes and the opaque minerals are designated as unstable, relatively stable and stable heavy minerals (Xiubin, Keli & Xiangyi, 1997). The values of  $K_1$  and  $K_2$  reflect both the degree of weathering in the source region and the degree of post-depositional pedogenetic alteration of the loess. Our results indicate that  $K_1$  and  $K_2$  cannot be used to establish any differences. However, the values of  $K_3$  reflect the uniformity in the loessic material and not weathering processes that occurred during the climatic optimum of the Holocene.

In addition, chemical data (Ca, Na, K, Mg, Cr, Ti, Mn, Fe and Zn contents) are displayed using a box and whisker plot (Fig. 6), a histogram-like method that helps us to interpret the distribution of data. In this plot, each box encloses the middle 50%,

where the median is represented as a horizontal line inside the box. Vertical lines extending from each end of the box (called whiskers) enclose data within 1.5 interquartile ranges. Values falling beyond the whiskers, but within three interquartile ranges, are plotted as individual points (suspect outliers). Far outside points (outliers) are distinguished. Ca has the highest concentration, with average concentration values of  $2 \times 10^5 \mu\text{g g}^{-1}$ , and the highest dispersion in the Villamejor (e group) and Villarrubia de Santiago (x group) samples. In general, concentration values for Na are very dispersed, especially in the Yepes samples (y group). This is the same situation for Ti and Mg in samples from Villarrubia de Santiago (x group). The K concentration values are about  $2 \times 10^4 \mu\text{g g}^{-1}$  with high dispersions in the Viloría river (a group) and Ontígola (t group) samples. These groups also present the highest concentrations for Fe together with the Zarza de Tajo samples (z group). The element Cr is characterized by a high dispersion in the Mesa de Ocaña (o group), Ontígola (t group) and Zarza de Tajo (z group) samples, and it can be mentioned that the values are below the quantification limit for Zn in the Villamejor (e group) samples.

In order to discern if there are significant differences in chemical and mineralogical (bulk sample and clay and sand fractions) composition between loess

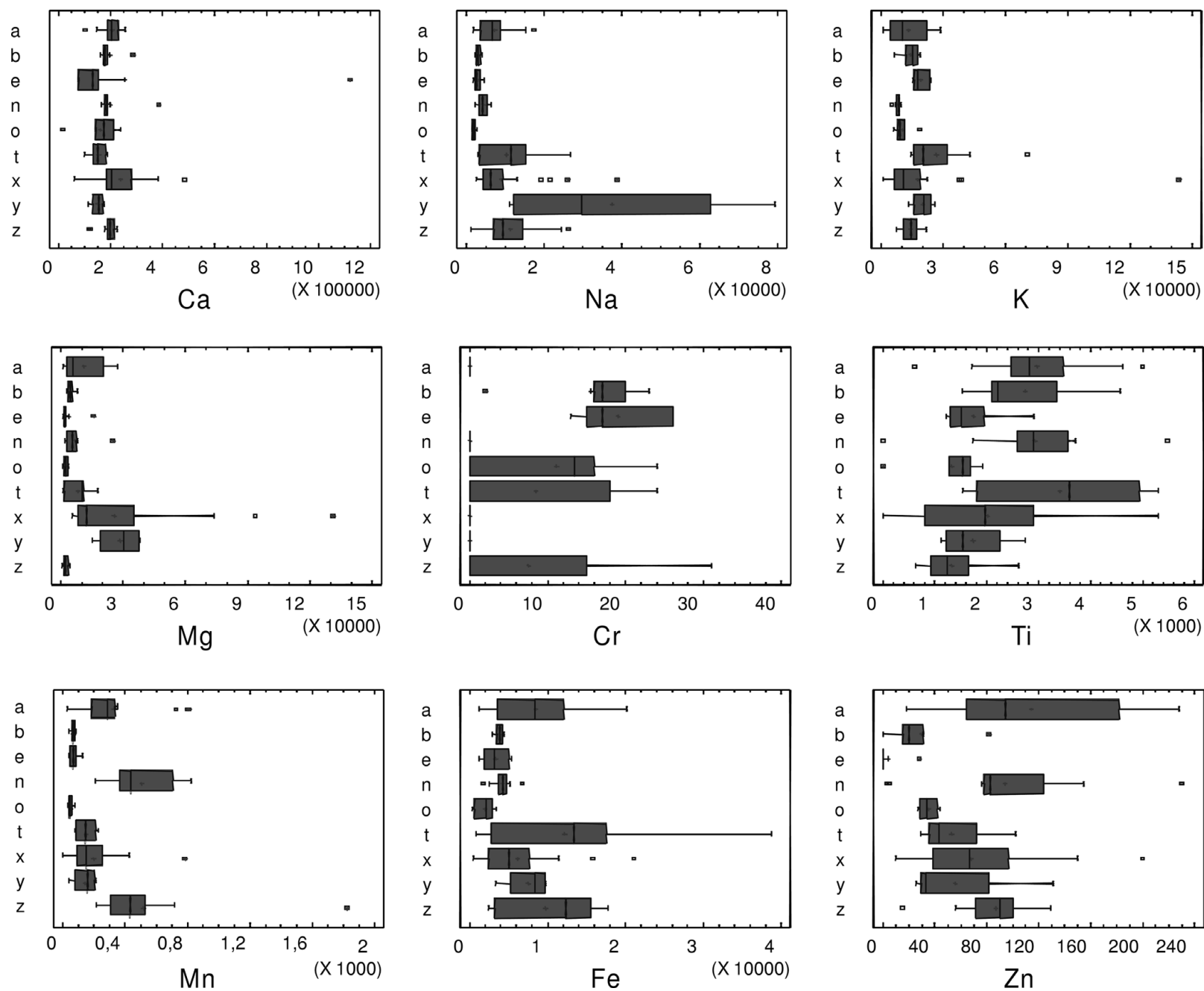


Figure 6. Box and whisker plot of the chemical elements analysed (a – Viloría stream; b – Ciruelos; e – Villamejor; n – Noblejas; o – Mesa de Ocaña; t – Ontígola; x – Villarrubia de Santiago; y – Yepes; z – Zarza de Tajo). Concentrations are expressed in  $\mu\text{g g}^{-1}$ . See <http://journals.cambridge.org/geo> for a colour version of this figure.

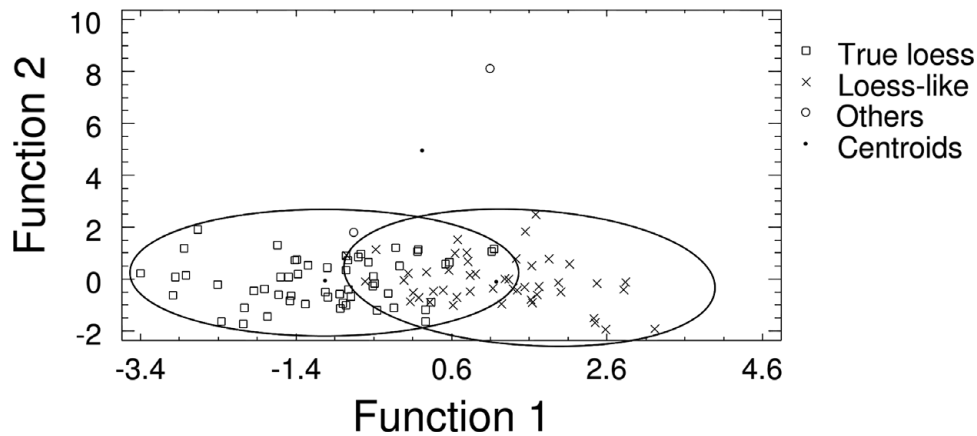


Figure 7. Chemical and mineralogical discriminant functions for 'true loess', 'loess-like' deposits and other unclassified samples. See <http://journals.cambridge.org/geo> for a colour version of this figure.

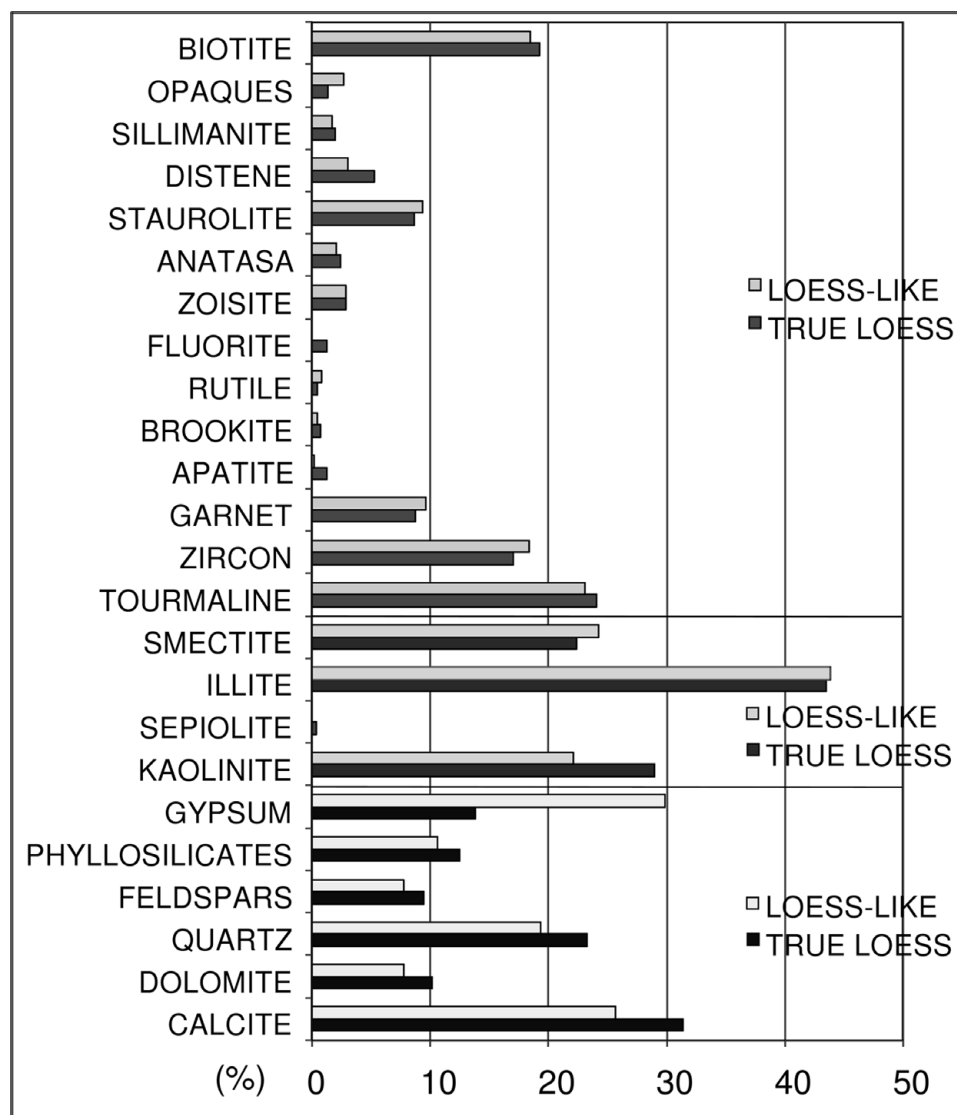


Figure 8. Variation in mineralogical composition of the sandy fraction, clay fraction and bulk sample for 'true loess' and 'loess-like' deposits of the different locations. See <http://journals.cambridge.org/geo> for a colour version of this figure.

considered 'true loess' or 'loess-like', discriminant analysis was used to help us in this purpose. The corresponding linear discriminant analysis is represented in Figure 7. For this study, 24 mineral variables (calcite,

dolomite, quartz, feldspars, phyllosilicates, gypsum, kaolinite, sepiolite, illite, smectite, tourmaline, zircon, garnet, apatite, brookite, rutile, fluorite, zoisite, anatase, staurolite, distene, sillimanite, opaques and



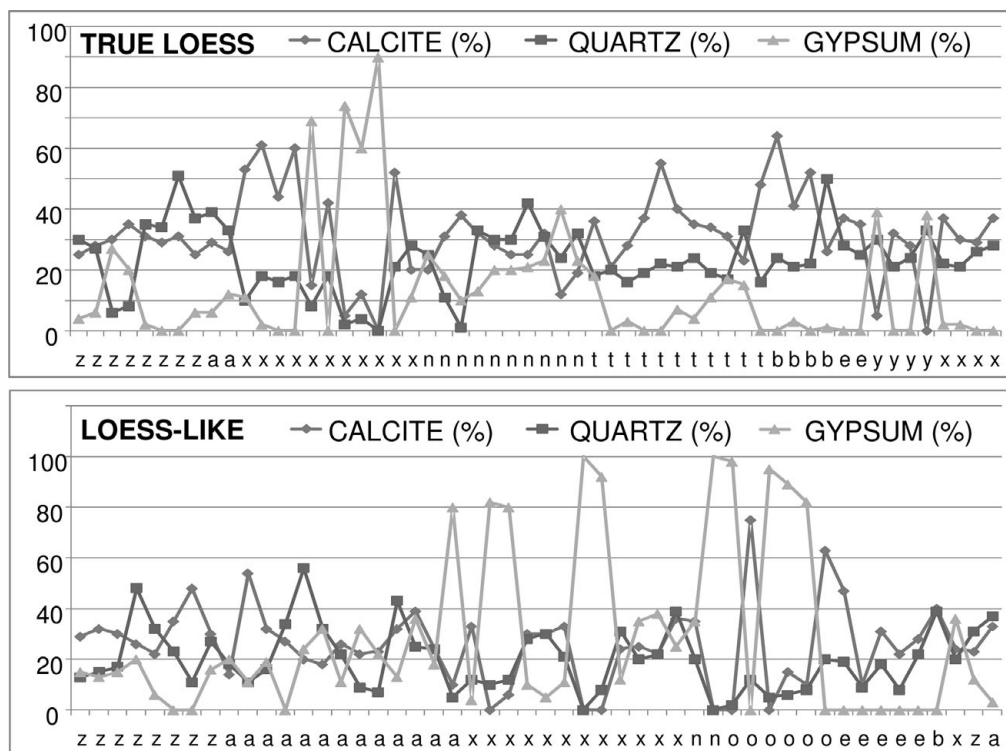


Figure 9. Variation of major mineral concentrations in ‘true loess’ and ‘loess-like’ deposits. See <http://journals.cambridge.org/geo> for a colour version of this figure.

biotite) and 10 chemical variables (Mn, Fe, Cu, Zn, Ti, Cr, Mg, Ca, Na and K) were considered. F1 represents 71.60% of the variance and F2 28.40%. These functions with *P*-values less than 0.05 are statistically significant at the 95% confidence level. F1 and F2 consider all the coefficients standardized (one coefficient positive and the other negative) except for smectite, brookite, rutile, zoisite and Mn (F1 and F2 are positive) and for tourmaline, fluorite, Zn, Mg and Na (F1 and F2 are negative). In this figure we can easily distinguish two different groups (‘true loess’ and ‘loess-like’) with a mixed zone where contamination has taken place due to the dominant winds of these zones. The bulk of the samples are located between the +2 and -2 values of standardized coefficients of F2, with F1 being the best function to discriminate among ‘true loess’ (located in the negative part of *x*-axis) and ‘loess-like’ (located in the positive part of *x*-axis).

Figure 8 represents the mineralogical composition of the bulk sample and clay and sand fractions. An interesting contrast can be observed between the ‘true loess’ and ‘loess-like’ samples. The greatest differences are in kaolinite concentration (higher in ‘true loess’) and in gypsum concentration (higher in ‘loess-like’ deposits); the rest of the light minerals also have a higher content in the ‘true loess’.

The variation in concentration of the most abundant mineral phases (quartz, calcite and gypsum) is represented in Figure 9, where the most representative mineral is gypsum with high concentrations in samples of ‘true loess’ from the Zarza de Tajo (x group) location and

‘loess-like’ deposits from the Zarza de Tajo and Mesa de Ocaña (o group) locations.

### 5. Conclusions

Loess deposits from the Spanish central region have a local origin. They are constituted by fine materials and characterized by a constant and uniform sedimentation. Their mineralogical and chemical characteristics are homogeneous and typical of the geomorphological and geological units located in the surroundings. However, some differences in their geomorphology and their chemical and mineralogical composition allow a differentiation between ‘true loess’ and ‘loess-like’ deposits as well as the role of western winds in the sedimentation of these aeolian loessic accumulations. In this sense, ‘true loess’ is accumulated on western slopes of valleys in a leeward position.

The role of cold climate environments seems to be indispensable in the formation of loess deposits as well as the wind action and lack of ground cover. The effects of drought are also important, as suggested by the location of the loess deposits in the area with less rainfall at present in central Spain.

Regarding chemical composition, similar concentrations of Ca, K, Mg and Na were found in all the samples, although it is important to note the higher concentration of Na in deposits located in the more western section due to deflation actions of western winds. The winds are capable of transporting fine materials from the Zócalo Toledano platform, which is rich in feldspars composed of calcium and sodium.

With respect to mineralogical composition, there are also some differences among samples. 'True loess' has the higher concentration of quartz, calcite and kaolinite. This suggests an allochthonous origin from deflation processes over alluvial sediments (terraces and flood plains) of the Tajo River and its tributaries. In this sense, 'true loess' from the interior of the Iberian Peninsula has quartz percentages similar to other loessic accumulations from the western Mediterranean, such as Italy, 60 %, (Cremaschi, 1987) or Tunisia, 30–65 %, (Coudé-Gausson & Rognon, 1988).

Loess deposits are better collected in the S–N-lying valleys, especially in asymmetric valleys, in relation to the western winds that determine the sedimentation.

On the other hand, the presence of gypsum in 'loess-like' deposits reaches average values twice as high as in 'true loess' due to different geomorphological processes that have occurred in both accumulations.

The indices of heavy minerals such as  $K_3$  reflect the minimal weathering processes in the source areas and after accumulation of the loess.

## References

- BISCAYE, P. E., GROUSSET, F. E., REVEL, M., VAN DER GAAST, S., ZIELINSKI, G. A., VAARS, A. & KUKLA, G. 1997. Asian provenance of glacial dust (stage 2) in the Greenland Ice Sheet Project 2 Ice Core, Summit, Greenland. *Journal of Geophysical Research* **102**, 26765–81.
- BRUNNACKER, K. 1969a. Observations en Espagne et en Grèce. *Supplement au Bulletin de l'Association Française pour l'étude du Quaternaire*, 67–9.
- BRUNNACKER, K. 1969b. Affleurements de loess dans les régions nord-méditerranées. *Revue Géographie Physique et Géologie Dynamique* **2**(11), 325–34.
- BRUNNACKER, K. & LÖZEK, V. 1969. Lössorkanmen in Südostspanien. *Zeitschrift für Geomorphologie NF* **13**, 297–316.
- COUDÉ-GAUSSON, G. 1991. *Les Poussières Sahariennes*. Paris, France: John Libbey Eurotext, 167 pp.
- COUDÉ-GAUSSON, G. 1998. Les loess peridésertiques de Matmata (Sud-Tunisien). *Géochronique* **65**, 11–12.
- COUDÉ-GAUSSON, G., HILLAIRE-MARCEL, C. & ROGNON, P. 1982. Origine et évolution pédologique des fractions carbonatées dans les loess de Matmata (Sud-Tunisien) d'après leurs teneurs en  $^{13}\text{C}$  et  $^{18}\text{O}$ . *Comptes Rendues Academie Sciences Françaises* **295**, 939–42.
- COUDÉ-GAUSSON, G., LE COUSTUMER, M. N. & ROGNON, P. 1984. Paléosols d'âge Pléistocène supérieur dans les loess des Matmata (Sud – Tunisien). *Sciences Géologiques de Strasbourg* **37**(4), 359–86.
- COUDÉ-GAUSSON, G., ROGNON, P., RAPP, A. & NIHLEN, T. 1987. Dating of peridesert loess in Matmata, south Tunisia, by radiocarbon and thermoluminescence methods. *Zeitschrift für Geomorphologie NF* **31**, 129–44.
- COUDÉ-GAUSSON, G. & ROGNON, P. 1988. The Upper Pleistocene loess of southern Tunisia: a statement. *Earth Surface and Process Landforms* **13**, 137–52.
- CREMASCHI, M. 1987. Loess deposits of the Plain of the Po and of the adjoining Adriatic Basin (Northern Italy). In *Loess and Periglacial Phenomena* (eds M. Pecsí & H. M. French), pp. 35–40. Budapest: Akademia Kiadó.
- CUENCA PAYÁ, A. & WALTER, M. J. 1976. Pleistoceno final y Holoceno en la cuenca del Vinalopó (Alicante). *Estudios Geológicos* **32**, 95–104.
- EBERL, D. D. & SMITH, D. B. 2009. Mineralogy of soils from two-continental scale transects across the United States and Canada and its relation to soil geochemistry and climate. *Applied Geochemistry* **24**(8), 1394–404.
- FRAZEE, C. J., FEHRENBACHER, J. B. & KRUMBEIN, W. C. 1970. Loess distribution from a source. *Soil Science Society American Proceedings* **34**, 296–301.
- GARCÍA, R., VIGIL, R. & GONZÁLEZ, J. A. 1998. *Periglacial loess fields in the Tajo River Valley, Spain*. Abstract. 17th General Meeting International Mineralogy Association, Toronto, Canada.
- GARCÍA GIMÉNEZ, R. & GONZÁLEZ MARTÍN, J. A. 2006. Los loess del Valle medio del río Tajo (Villarrubia de Santiago-Yepes, España). *Boletín Real Sociedad Española de Historia Natural (Sección Geología)* **101**, 51–78.
- GARCÍA, R., GONZÁLEZ, J. A., PETIT, M. D. & RUCANDIO, M. I. 2010. Caracterización de las acumulaciones loésicas en el Valle medio del Río Tajo, España. *Estudios Geológicos* **66**, 115–21.
- GOUDIE, A. S. & MIDDLETON, N. J. 2001. Saharan dust storms: nature and consequences. *Earth Science Review* **56**, 179–204.
- GRUNERT, J. & LEHMKUHL, J. F. 2004. Aeolian sedimentation in arid and semiarid environments of Western Mongolia. In *Paleoecology of Quaternary Drylands. Lecture Notes in Earth Sciences vol. 102* (eds W. P. Smykatz-Kloss & P. Felix Henningsen), pp. 195–218. Berlin: Springer.
- GÜNSTER, N., ECK, P., SKOWRONEK, A. & ZÖLLER, L. 2001. Late Pleistocene loess and their paleosols in the Granada Basin, Southern Spain. *Quaternary International* **76/77**, 241–5.
- HAASE, D., FINK, J., HAASE, G., RUSKE, R., PECSI, M., RICHTER, H., ALTERMANN, M. & JÄGER, K. D. 2007. Loess in Europe – its spatial distribution based on a European Loess Map, scale 1:2,500,000. *Quaternary Science Review* **26**, 1301–12.
- HEY, R. W. 1972. The Quaternary and Paleolithic of northern Libya. *Quaternaria* **6**, 435–49.
- JIN, Z., YOU, C. & YU, J. 2009. Toward a geochemical mass balance of major elements in Lake Qinghai, NE Tiberan Plateau: a significant role of atmospheric deposition. *Applied Geochemistry* **24**(10), 1901–7.
- KISCH, H. 1990. *Recommendations on Illite Crystallinity*. IGCP Project 294, VIGM, pp. 1–9.
- MOORE, D. M. & REYNOLDS, D. C. JR. 1997. *X-ray Diffraction and the Identification and Analysis of Clay Minerals*, 2nd ed. New York: Oxford University Press, 238 pp.
- ORDOÑEZ, S., LÓPEZ-AGUAYO, F. & GARCÍA DEL CURA, M. A. 1977. Contribución al conocimiento de la mineralogía del yacimiento de sales de Villarrubia de Santiago (Toledo). *Estudios Geológicos* **33**, 167–71.
- PECSI, M. 1990. Loess is not just the accumulation of dust. *Quaternary International* **7/8**, 1–21.
- PÉREZ GONZÁLEZ, A., SILVA, P. G., ROQUERO, E. & GALLARDO, J. 2004. Geomorfología fluvial y edafología del sector meridional de la cuenca de Madrid (Toledo-Madrid). In *Itinerarios geomorfológicos por Castilla la Mancha* (eds G. Benito & A. Díez Herrero), pp. 31–9. Madrid, Spain: Sociedad Española de Geomorfología.
- PYE, K. 1995. The nature, origin and accumulation of loess. *Quaternary Science Review* **14** (7–8), 653–67.

- ROSE, J., MENG, X. & WATSON, C. 1999. Paleoclimate and paleoenvironmental responses in the western Mediterranean over the last 140 ka. Evidence from Mallorca, Spain. *Journal Geological Society* **156**, 435–48.
- RUIZ ZAPATA, M. B., PÉREZ GONZÁLEZ, A., DORADO, M., VALDEOLMILLOS, A., BUSTAMANTE, I. & GIL, M. J. 2000. Caracterización climática de las etapas áridas del Pleistoceno superior en la región central peninsular. *Geotemas* **1**(4), 273–8.
- SCHULTZ, L. G. 1964. *Quantitative Interpretation of the Mineralogical Composition from X-ray and Chemical Data for the Pierce Shale*. United States Geological Survey Professional Paper, 391C, 131 pp.
- SMALLEY, I. 1995. Making the material: the formation of silt-sized primary mineral particles for loess deposits. *Quaternary Science Review* **14**, 645–51.
- TAYLOR, S. R., MCLENNAN, S. M. & MCCULLOCH, M. T. 1983. Geochemistry of loess, continental crustal composition and crustal model ages. *Geochimica and Cosmochimica Acta* **47**, 1897–905.
- WHALLEY, W. B., MARSHALL, J. R. & SMITH, B. J. 1982. Origin of desert loess from some experimental observations. *Nature* **300**, 433–5.
- XIUBIN, H., KELI, T. & XIANGYI, L. 1997. Heavy mineral record of the Holocene environment on the Loess Plateau in China and its pedogenetic significance. *Catena* **29**, 323–32.